HYDROLOGICAL PROCESSES
Hydrol. Process. **13**, 2423–2438 (1999)

A distributed model of blowing snow over complex terrain

Richard Essery,[1] Long Li[1] and John Pomeroy[2]*
[1]*Division of Hydrology, University of Saskatchewan, Saskatoon, Saskatchewan, Canada, S7N 0W0*
[2]*National Hydrology Research Centre, Saskatoon, Saskatchewan, Canada S7N 3H5*

Abstract:

Physically-based models of blowing snow and windflow are used to develop a distributed model of blowing snow transport and sublimation over complex terrain. The model is applied to an arctic tundra basin. A reasonable agreement with results from snow surveys is obtained, provided sublimation processes are included; a simulation without sublimation produces much greater snow accumulations than were measured. The model is able to reproduce some observed features of redistributed snowcovers: distributions of snow mass, classified by vegetation type and landform, can be approximated by lognormal distributions, and standard deviations of snow mass along transects follow a power law with transect length up to a cut-off. The representation used for the downwind development of blowing snow with changes in windspeed and surface characteristics is found to have a large moderating influence on snow redistribution. Copyright © 1999 John Wiley & Sons, Ltd.

KEY WORDS blowing snow; snow transport; sublimation; snow distribution; snow surveys; complex terrain

INTRODUCTION

Large amounts of wind-blown snow can sublimate in open environments, and redistribution of snow by wind can lead to large variations in depth which influence the depletion of snow during melt (Donald *et al.*, 1995; Shook, 1995). Transport and sublimation rates increase rapidly with increasing windspeed and so are highly sensitive to windspeed variations caused by variations in topography and roughness. In this paper, results from the Prairie Blowing Snow Model (Pomeroy, 1988; Pomeroy *et al.*, 1993; Pomeroy and Li, 1999a) and the MS3DJH/3R terrain windflow model (Walmsley *et al.*, 1982, 1986; Taylor *et al.*, 1983) are used to develop a distributed model of blowing snow over complex terrain. The model is applied to Trail Valley Creek, an arctic tundra basin 50 km north of Inuvik, NWT, using half-hourly meteorological data. Such frequent measurements, although valuable for modelling non-linear blowing snow processes, are rarely available for arctic locations; previous distributed blowing snow models have been driven with monthly (Pomeroy *et al.*, 1997) or daily (Liston and Sturm, 1998) data.

The Prairie Blowing Snow Model (PBSM) is a physically-based model that calculates transport and sublimation rates for blowing snow over uniform terrain given measurements of air temperature, humidity and windspeed. Data requirements and the complexity of its algorithms make PBSM unsuitable for use in distributed models, so a simplified blowing snow model ('SBSM'), which can reproduce PBSM results very closely with much less computational effort, is used. The requirement for distributed meteorological data is addressed, in part, by using MS3DJH/3R to produce windflow maps; other atmospheric variables are assumed to be homogeneous over the model domain. Lacking a physically-based model of blowing snow

* Correspondence to: John Pomeroy, National Hydrology Research Centre, Saskatoon, Saskatchewan, Canada, S7N 3H5.

CCC 0885–6087/99/142423–16$17·50

Received 7 October 1998
Revised 4 January 1999
Accepted 11 March 1999

Table I. Coefficients of variation in late-winter snow mass for various arctic vegetation types and landforms, reproduced for Pomeroy *et al.* (1998)

Vegetation	Landform	C_v
Tundra	Flat plains, upland plateaux	0·31
	Valley bottoms	0·28
	Valley sides (drifts for slopes $> 9°$)	0·34
Shrub tundra	Flat plains	0·22
	Valley bottoms	0·16
	Valley sides (drifts for slopes $> 9°$)	0·18
Sparse forest-tundra	Exposed hillside and forest edge	0·21
	Sheltered	0·11

development in response to small-scale spatial variations in windspeed and surface characteristics, we have adopted an *ad hoc* representation, consistent with available measurements (Takeuchi, 1980), and investigated the sensitivity of simulations to its inclusion; the development of blowing snow fluxes over homogeneous fetches is a problem of current theoretical interest (Déry *et al.*, 1998).

Observed snow depths or masses for a redistributed snowcover can often be approximated by a lognormal distribution (Donald *et al.*, 1995; Shook, 1995; Pomeroy *et al.*, 1998), characterized by a mean and a coefficient of variation (standard deviation divided by mean). Vegetation and topography influence the redistribution of snow (Pomeroy and Gray, 1995), so different vegetation types and landforms can be expected to have snow distributions with different parameters, and stratified sampling techniques are required to obtain accurate estimates of area-average snow masses for complex terrains (Steppuhn and Dyck, 1974). Table I, reproduced from Pomeroy *et al.* (1998), gives coefficients of variation (C_v) in snow mass collated from late-winter snow surveys for arctic landscapes with various vegetation types and landforms. C_v tends to be small for tall, dense vegetation and sheltered locations with little redistribution of snow, and greater for landforms which cause windflow divergence and consequent erosion and deposition of snow.

Expected standard deviations for data drawn from random distributions do not depend on sample size, but snow depths at adjacent points are not randomly distributed, and instead are correlated over some distance. The standard deviation of depths measured along a transect thus increases with transect length up to this distance and approaches a constant value for larger distances, showing a transition to random behaviour. Shook and Gray (1996) found measured snow depths to have fractal characteristics on small scales; that is, for a range of sample length l, the standard deviation is proportional to l^H for some H — the 'Hausdorff dimension' (Turcotte, 1992) — which can be estimated by fitting a straight line to a log–log plot of average standard deviation against sample length. If the standard deviation approaches a constant value for large sample lengths, a cut-off length for the fractal behaviour can be defined from the intersection of the fractal curve and the asymptote.

As an illustration, Figure 1(a) shows snow depths measured on 10 March 1998 and approximate elevations along a 2·3 km north–south transect crossing Trail Valley Creek (TVC). A snow depth frequency histogram for the measurements is shown in Figure 1(b) and compared with a lognormal distribution; the mean and coefficient of variation for this distribution were calculated excluding measurements made on the deep drift near the foot of the north-facing slope, which otherwise skew the distribution. Average standard deviations obtained by dividing the transect into shorter samples are shown in Figure 1(c). Comparison with the fitted line shows that the standard deviation closely follows a power law with sample length. The increase in standard deviation is weak ($H = 0{\cdot}1$), but shows no sign of leveling off over the length of the transect. From previous TVC snow surveys, Shook and Gray (1996) found $H = 0{\cdot}3$ and suggested a cut-off length of 500 m. In contrast, for surveys on a flat prairie field they found a much shorter cut-off length of 20 m and $H = 0{\cdot}47$.

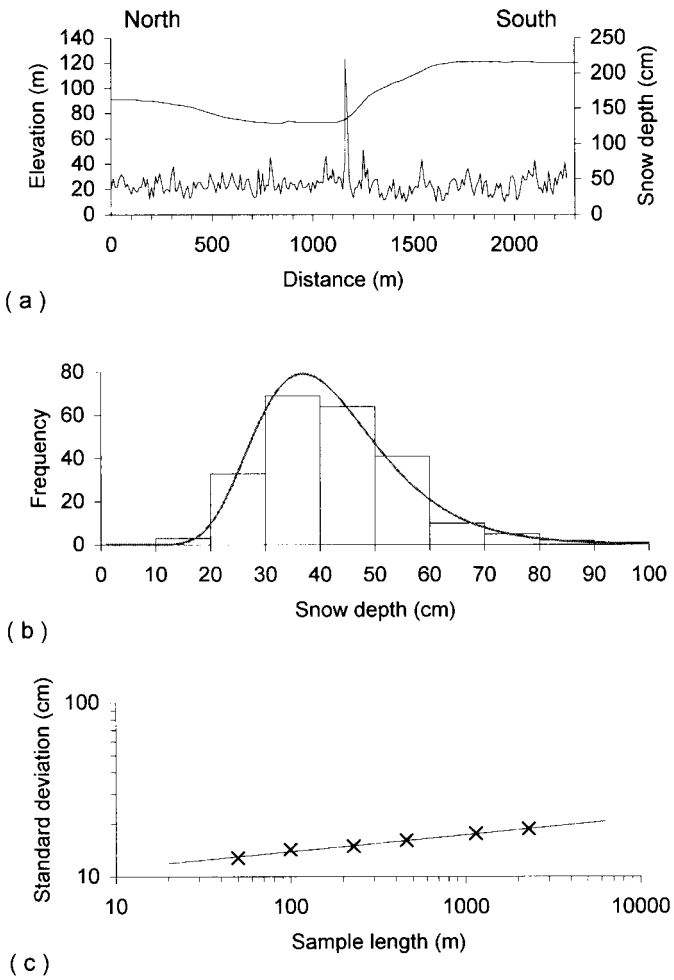

Figure 1. Results from measurements of snow depth on a north–south transect crossing TVC. (a) Snow depth (lower line) and elevation along the transect. (b) Frequency histogram for the depths shown in (a), compared with a lognormal distribution. (c) Average standard deviation of snow depth for samples of length l. The fitted line is proportional to $l^{0.1}$.

SIMPLIFIED BLOWING SNOW MODEL

The rate of mass transport by blowing snow across a unit width perpendicular to the wind is given by

$$Q_T = Q_{salt} + \int_{h_*}^{Z_b} \eta(z)u(z)dz \tag{1}$$

where Q_{salt} is the rate of transport by saltation in a layer of depth h, near the surface, $u(z)$ is the windspeed at height z and $\eta(z)$ is the mass concentration of suspended snow, which increases with windspeed but decreases with height. The upper boundary for suspended snow, z_b, increases with windspeed, surface roughness and downwind distance.

Despite the complexity of the terms in equation (1), it turns out that PBSM gives transport rates that scale approximately as the fourth power of windspeed, with a weak dependence on air temperature through the threshold windspeed at which blowing snow commences; PBSM uses a quadratic function of temperature derived from observations of blowing snow occurrence to calculate this threshold (Li and Pomeroy, 1997a).

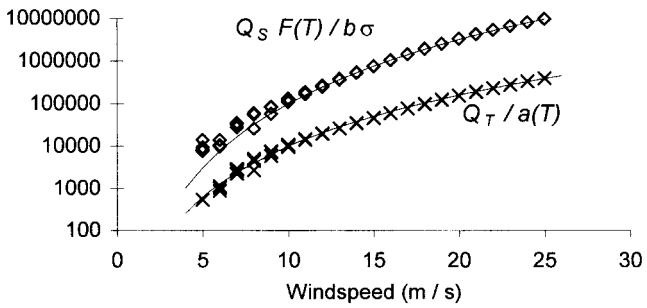

Figure 2. Scaled transport (X) and sublimation (◇) rates from PBSM for temperatures between −40 °C and 0 °C and relative humidities of 70 percent and 90 percent. The fitted curves are u^4 and u^5

In place of the numerical integration used by PBSM to evaluate equation 1, SBSM thus uses an approximation of the form

$$Q_T = a(T)u_{10}^4, \tag{2}$$

where u_{10} (m s^{-1}) is the windspeed at a height of 10 m, T (°C) is the air temperature, and the temperature function

$$a(T) = (1710 + 1{\cdot}36T) \times 10^{-9} \tag{3}$$

is fitted to PBSM results. Figure 2 shows how PBSM transport rates, divided by $a(T)$, depend on windspeed over a 1000 m fetch of complete snowcover without exposed vegetation; the fitted line shows that equation 2 gives a good approximation.

PBSM calculates the rate of sublimation from blowing snow over a unit area of ground as

$$Q_S = \int_0^{z_b} \frac{1}{\bar{m}(z)} \frac{d\bar{m}}{dt} \eta(z) dz, \tag{4}$$

where $\bar{m}(z)$ is the average blowing snow particle mass at height z, calculated assuming that particle sizes follow a gamma distribution (Schmidt, 1982). For air temperature T and undersaturation σ, Thorpe and Mason (1966) give an expression for the rate of mass decrease for a snow particle of mass m and radius r that can be written in the form

$$\frac{dm}{dt} = 2\pi r\ Nu \frac{\sigma}{F(t)}, \tag{5}$$

where Nu is the Nusselt number and

$$F(T) = \frac{L_s}{\lambda_T(T + 273)} \left[\frac{L_s M}{R(T + 273)} - 1 \right] + \frac{1}{D\rho_s}. \tag{6}$$

$F(T)$ only depends on temperature; L_s is the latent heat of sublimation, M is the molecular weight of water, R is the universal gas constant, λ_T is the thermal conductivity of air, D is the diffusivity of water vapour in air and ρ_s is the water vapour saturation density. PBSM includes a second term in equation 5 to allow for shortwave radiation absorbed by snow particles (Schmidt, 1991) but this typically only adds a small

correction; neglecting this term, and using the PBSM assumption that the undersaturation at any height is proportional to σ_2, the undersaturation at 2 m, equation 4 can be written as

$$Q_s = \frac{\sigma_2}{F(T)} Q_s^l, \tag{7}$$

where Q_s^l is a scaled sublimation rate. Figure 2 shows that, for a 1000 m fetch, PBSM gives scaled sublimation rates proportional to u_{10}^5 but with little dependence on temperature or humidity. SBSM thus replaces the numerical integration of equation 4 with an approximation

$$Q_s = \frac{b\ \sigma_2}{F(T)} u_{10}^5, \tag{8}$$

where b is a constant.

To scale from a point to a uniform area, PBSM weights blowing snow fluxes by the probability of blowing snow occurrence (Pomeroy and Li, 1999a). Li and Pomeroy (1997b) found this probability to follow a cumulative normal distribution

$$P(u_{10}) = \frac{1}{\sqrt{2\pi}\delta} \int_0^{u_{10}} \exp\left\{-\frac{(\bar{u} - u)^2}{2\delta^2}\right\} du, \tag{9}$$

where, for dry snow of age A (in hours), the parameters of the distribution are given by

$$\bar{u} = 11{\cdot}2 + 0{\cdot}365T + 0{\cdot}00706T^2 + 0{\cdot}9\ \ln(A) \tag{10}$$

and

$$\delta = 4{\cdot}3 + 0{\cdot}145T + 0{\cdot}00196T^2. \tag{11}$$

For wet or icy snow, the parameters are taken to be $\bar{u} = 21$ m s^{-1} and $\delta = 7$ m s^{-1}.

Equation 9 can be expressed as a sum of two error functions. Since most compilers do not supply intrinsic error functions, PBSM uses a numerical integration to obtain $P(u_{10})$, but the cumulative normal distribution can also be approximated by

$$P(u_{10}) = \left[1 + \exp\left\{\frac{\sqrt{\pi}(\bar{u} - u_{10})}{\delta}\right\}\right]^{-1}. \tag{12}$$

Figure 3 compares equation 12 with numerical integrations of equation 9.

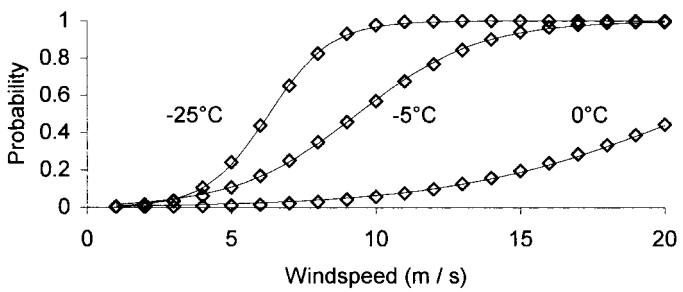

Figure 3. Probability of blowing snow occurrence from equation 8 (◇) and equation (11) (—)

If vegetation extends above the snow, the surface wind stress is partitioned between the snow surface and the protruding vegetation. Using a stress-partitioning relationship due to Raupach *et al.* (1993), u_{10} in equation 12 is replaced by

$$u_s = \frac{u_{10}}{(1 + 340 z_{ov})^{1/2}} \tag{13}$$

in this case, where z_{ov} is the exposed vegetation roughness length. Lettau (1969) gives

$$z_{ov} = \frac{Ndh}{2} \tag{14}$$

for vegetation of height h, stalk diameter d and stalk density N. Snow depths are subtracted from h to give exposed vegetation heights.

TERRAIN WINDFLOW MODEL

Windflow over complex terrain is modelled here using the MS3DJH/3R model developed by Walmsley and co-workers (Walmsley *et al.*, 1982, 1986; Taylor *et al.*, 1983) from theoretical work by Jackson and Hunt (1975) and Mason and Sykes (1979). Linearized momentum equations are solved using Fourier transforms of topography specified by a Digital Elevation Model (DEM). As a linear model, MS3DJH/3R is only valid for flow over low hills with slopes less than about 1 in 4 and assumes neutral stratification (studies of blowing snow generally assume that shear production of turbulence gives neutral stratification, but the suppression of turbulence by suspended snow has been considered by Bintanja, 1998).

Figure 4 shows elevations from a 40 m resolution DEM covering a 14 × 12 km area around TVC. Since the area that can be covered by MS3DJH/3R is limited, the TVC region was split into 42 cells of 128 × 128 gridpoints. To allow for adjustment to the periodic boundary conditions used by the model, the cells were overlapped and the central 50 × 50 gridpoints from each cell were combined to give windflow maps of the whole area. Simulated windspeeds, normalized to give area-averages equal to 1, are shown in Figure 5 for winds from the NW and SW; variations in windspeed highlight terrain features oriented perpendicular to the wind.

Surface roughness during blowing snow depends on windspeed and the height of exposed vegetation, but, although MS3DJH/3R can represent surfaces of variable roughness, a uniform roughness length of 0·005 m was assumed for the windflow simulations. This simplification removes the need to couple the windflow and blowing snow models; the distributed blowing snow model can simply read wind vectors from maps produced by the windflow model. Since the windflow model is linear and can be scaled by the observed windspeed, a single simulation is required for each incident wind direction. Simulations were performed for incident directions at 45 ° increments from 0° (north) to 315°, and observed wind directions were rounded to the nearest of these directions for the distributed blowing snow model. The coefficient of variation in windspeed is close to 0·06 for all directions, and is fairly insensitive to the value chosen for the surface roughness, scaling as $z_0^{0.06}$.

DISTRIBUTED BLOWING SNOW MODEL

Description

In the absence of melting, the rate of change in snow mass S at a point is

$$\frac{\partial S}{\partial t} = S_f - q_s - \nabla \cdot \boldsymbol{q}_t, \tag{15}$$

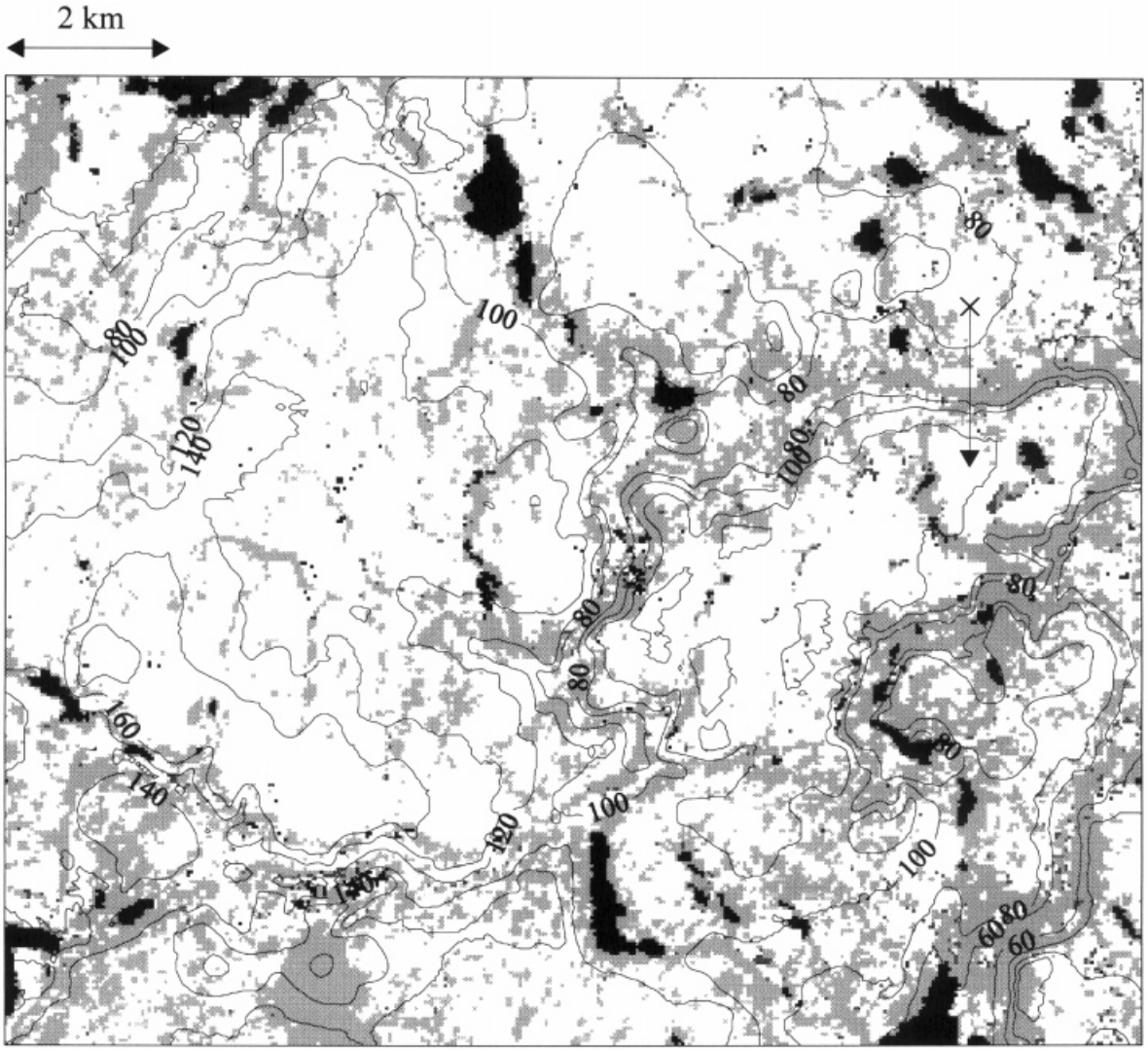

Figure 4. Elevation and vegetation maps for TVC. The vegetation classes are: lakes (black), open tundra (white), shrub tundra (light grey) and sparse forest (dark grey). The cross shows the location of the meteorological station and the line shows the course of the snow survey shown in Figure 1

where S_f is the snowfall rate, assumed to be homogeneous, q_s is the local sublimation rate and $\nabla \cdot \boldsymbol{q}_t$ is the rate of snow ablation or deposition by transport; the vector $\boldsymbol{q}_t$ is parallel to the local wind direction.

PBSM was developed for homogeneous fetches of 300 m or greater. To represent the downwind development of blowing snow in response to spatial variations in windspeed and surface characteristics on smaller scales, an *ad hoc* scheme, similar to that introduced by Liston and Sturm (1998), is used. Local fluxes are assumed to follow

$$q_{s,t} = P\, Q_{S,T} - \frac{F}{3}\boldsymbol{n} \cdot \nabla q_{s,t}, \tag{16}$$

where P is the probability given by equation 9, Q is the fully-developed flux for fetch $F = 1000$ m given by equation 2 or 8 and $\boldsymbol{n}$ is a unit vector parallel to the wind. For a step change in windspeed, this gives an

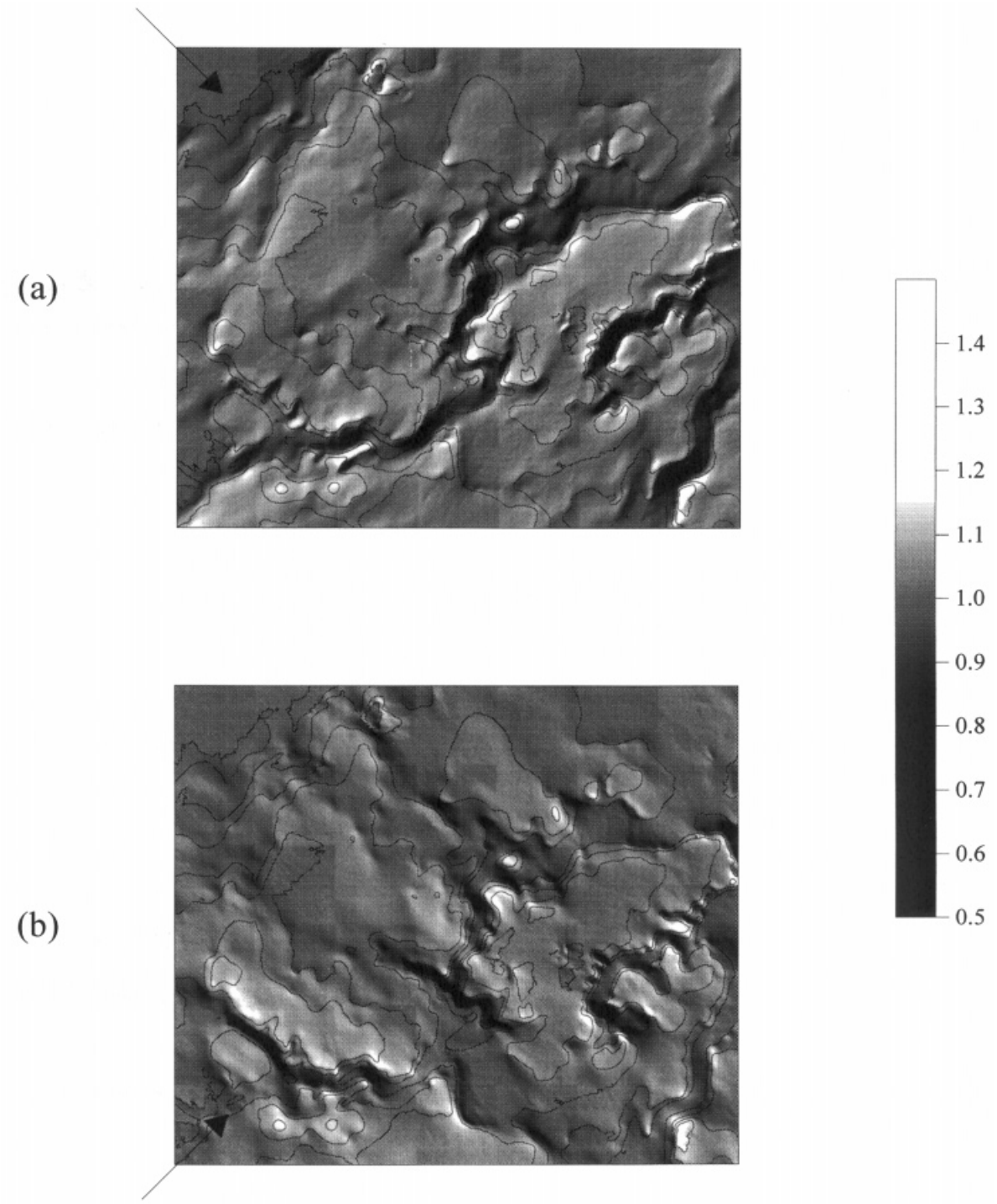

Figure 5. Normalized speeds for (a) NW and (b) SW winds

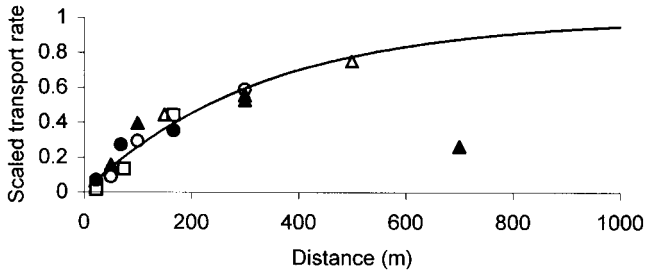

Figure 6. Fractional development of blowing snow fluxes with fetch from equation 15 with $F = 1000$ m (—) and measured transport rates (Takeuchi, 1980), scaled to the curve, for windspeeds of 5·2 (○), 7·2 (▲), 7·3 (△), 8·4 (●) and 8·7 (□) m s^{-1}

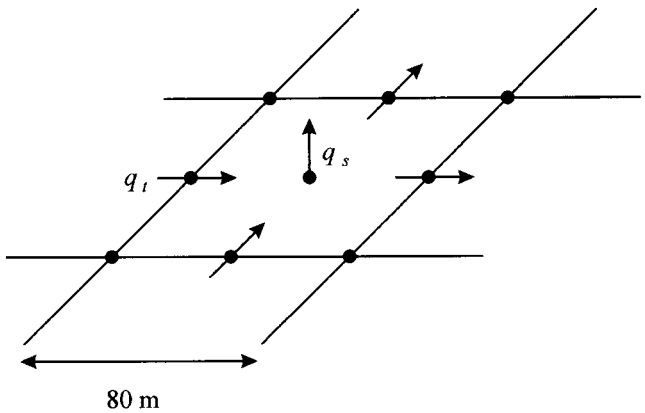

Figure 7. Schematic illustration of the spatial discretization used for the distributed snow mass balance, equation 15. Nodes represent windflow-model gridpoints and arrows represent snow mass fluxes

exponentially-decaying response completing 95% of the adjustment to full-development at the new windspeed in distance F. The fractional adjustment is shown in Figure 6 and compared with transport rates measured downwind of an ice-free river by Takeuchi (1980). Apart from one profile which showed a decrease in transport between distances of 300 m and 700 m, the measurements can all be scaled to fall close to the model curve.

The distributed blowing snow model uses a grid length twice that of the windflow model, dividing the TVC area into 26250 boxes of 80 × 80 m. Sublimation is calculated at the centre of each box and transport rates across the boundaries of the box are used in a central difference approximation for $\nabla \cdot \boldsymbol{q}_t$, illustrated in Figure 7. The probability calculated at the centre of a box is used to weight the sublimation from the box and the transport at its outflow boundaries. Upwind differences are used to evaluate the gradient term in equation 16; full development is assumed at inflow boundaries of the model domain.

Meteorological data and model parameters

Observations used to drive the distributed blowing snow model were made during the winter of 1996–1997 at an unattended meteorological station operated by the National Hydrology Research Institute. The location of the station is marked by a cross near the upper right corner of Figure 4. Air temperature, humidity, windspeed and direction were measured half-hourly using a calibrated Vaisala HMP35CF thermohygrometer and a Solent heated two-axis ultrasonic anemometer. Windspeeds from an NRG cup anemometer were used to cover periods when power for the ultrasonic anemometer failed. The high-quality windspeed record required for modelling blowing snow is difficult to obtain in harsh arctic environments; there are periods when neither anemometer was operational, the longest such period extending from 10 to

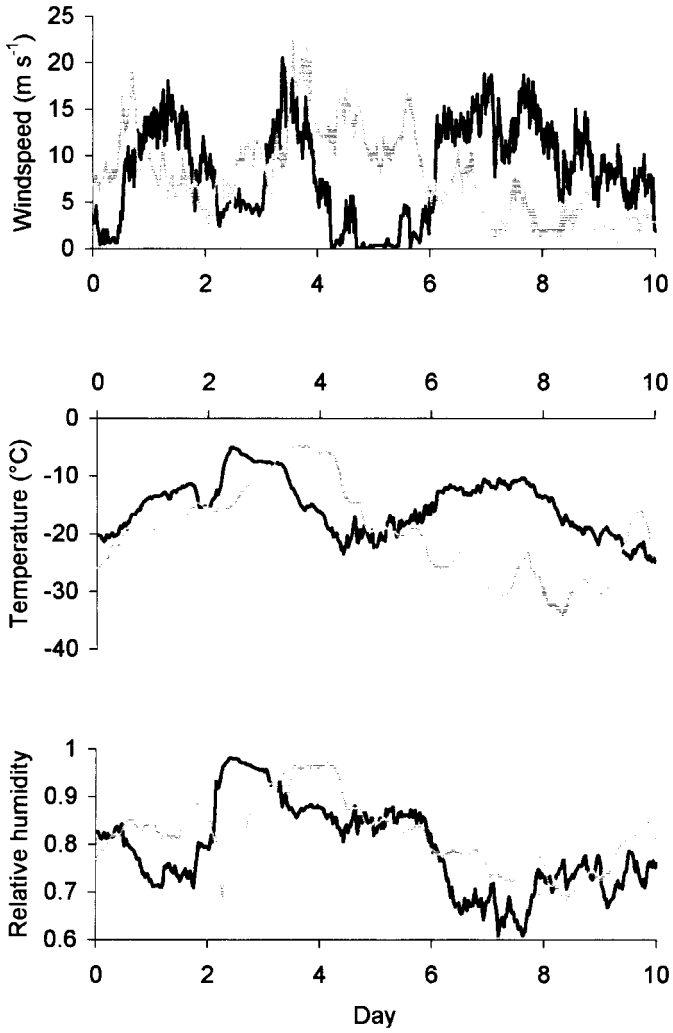

Figure 8. Observed windspeeds, temperatures and humidities for periods starting 9 November 1996 (black lines) and 10 March 1997 (grey lines)

22 December. The performance of PBSM in simulating snow accumulation at the station site over the latter part of this winter is discussed by Pomeroy and Li (1999b).

Snowfall was estimated using a Nipher-shielded snow gauge, emptied during four visits to the site and corrected for undercatch (Goodison *et al.*, 1998), and from the accumulation at a sheltered site believed to be uninfluenced by redistribution, sublimation, interception or melting of snow. Significant snowfall events were identified from changes in snowdepth measured by a Campbell SR50 ultrasonic sounder. Since snowfall rates were not measured, the cumulative snowfall was equally partitioned between snowfall events.

Modelled blowing snow fluxes are dominated by periods of high winds in mid-November 1996 and mid-March 1997; windspeeds, temperatures and humidities for these periods are shown in Figure 8. The simulated snow transport is dominated by northwesterly winds, but relatively dry and warm southerly winds in November also give significant sublimation.

In addition to topography, Figure 4 shows a vegetation map derived from a Landsat image of TVC (Pomeroy *et al.*, 1997). For use in the distributed blowing snow model, the vegetation was lumped into four

Table II. Vegetation parameters Nd and h for equation 14. S_v is the snow mass required to fill the roughness elements and z_{ov} is the snow-free roughness length for each vegetation class

Vegetation	Nd (m^{-1})	h (m)	S_v (kg m^{-2})	z_{ov} (m)
Lakes	0·2	0·01	2·4	0·001
Open tundra	0·1	0·08	19·2	0·004
Shrub tundra	0·1	1	240	0·05
Sparse forest	0·16	3	720	0·24

classes: lakes, open tundra, shrub tundra and sparse forest. Shrubs and trees in the valleys give way to open tundra on upland plains. Parameters chosen for each class, based on field surveys, are given in Table II. Corresponding snow masses required to fill the roughness elements, assuming a snow density of 240 kg m^{-3}, and snow-free roughness lengths are also shown. The lake parameters are intended to represent ice surface roughness and trapping of snow by white ice formation.

Results

The distributed blowing snow model was run for the 210-day period between 11 September 1996 and 8 April 1997; total snowfall was estimated as 179 kg m^{-2} for this period. Figure 9 shows the distribution of snow at the end of the simulation; vegetation clearly has a strong control on snow accumulation, areas of

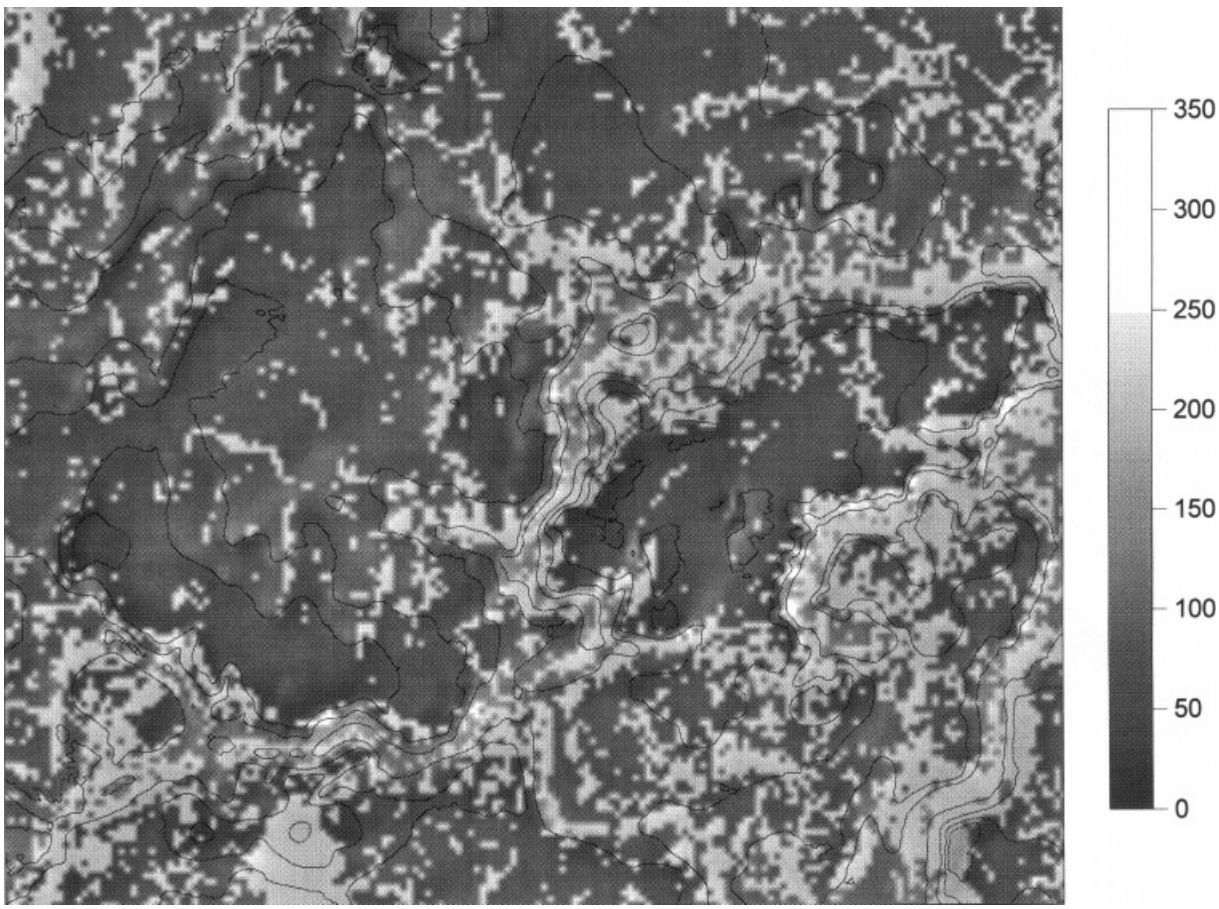

Figure 9. Simulated end-of-winter snow mass distribution (kg m^{-2})

Table III. Average snow mass and C_v for each vegetation class at the end of the simulation, and cumulative net transport and sublimation over the simulation period. Numbers in brackets are percentages of the estimated total snowfall (179 kg m^{-2})

Vegetation	Net transport (kg m^{-2})	Sublimation (kg m^{-2})	Average snow mass (kg m^{-2})	C_v
Lakes	−39 (−22%)	71 (40%)	69 (38%)	0·32
Open tundra	−32 (−18%)	85 (47%)	62 (36%)	0·42
Shrub tundra	80 (45%)	44 (25%)	215 (120%)	0·09
Sparse forest	105 (59%)	47 (26%)	237 (132%)	0·08

deep snow coinciding with tall vegetation (*cf.* Figure 4). Net transport, cumulative sublimation, average snow mass and C_v at the end of the simulation are given in Table III for each vegetation class, and the evolution of the snowcover through the simulation is shown in Figure 10. Net transport to shrubs and forests exceeds sublimation, so their average accumulation is greater than the snowfall. Lakes and open tundra are

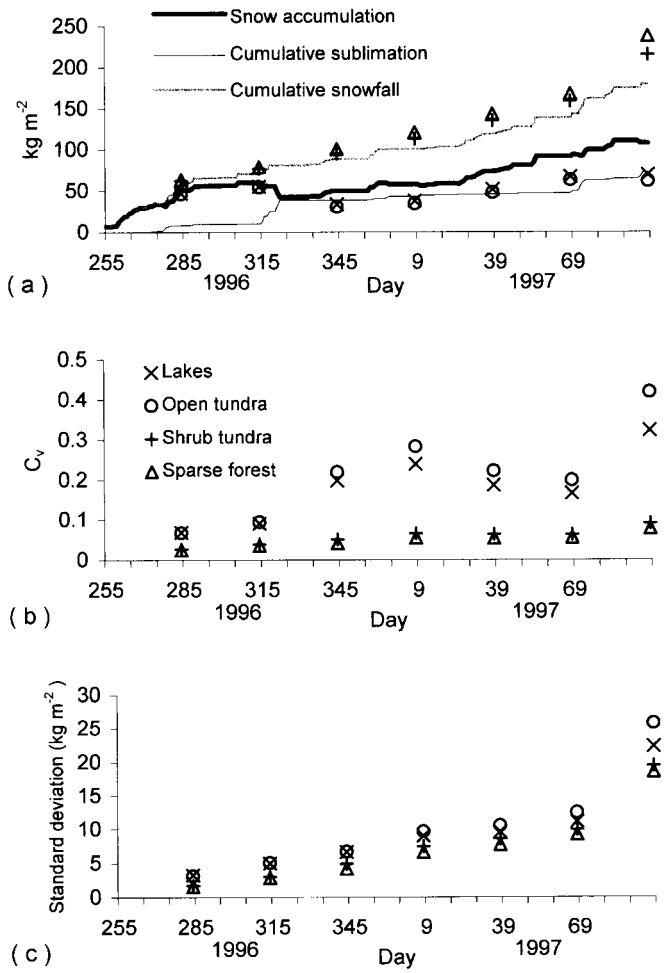

Figure 10. Simulated snowcover evolution. (a) Lines show cumulative snowfall, average snow mass and cumulative sublimation for the entire model domain. Markers show average snow masses for individual vegetation classes. (b) Coefficients of variation in snow mass for the vegetation classes. (c) Standard deviations of snow mass for the vegetation classes

Table IV. Results from snow surveys on 23 April 1997

Vegetation	Average snow mass ($kg\ m^{-2}$)	Standard deviation ($kg\ m^{-2}$)	C_v
Open tundra	86	27	0·31
Shrub tundra	219	42	0·19
Forest	215	49	0·23

sources of blowing snow; 47% of the snowfall on open tundra sublimates and a further 18% is lost to transport. Lakes are generally located in relatively sheltered low-lying areas and are fringed with shrubs which trap snow blowing from upwind areas, so lakes on average suffer less sublimation than open tundra but lose more snow through transport.

Simulated values of C_v are not strictly comparable with survey results (Blöschl, 1999), typically calculated from point measurements with spacings of a few metres, but they show the same decrease with increasing vegetation height. Late-winter C_v is observed to be fairly consistent from year to year for a given landscape, but Figure 10(b) shows that coefficients of variation are rather variable through the course of the simulation. Standard deviations, shown in Figure 10(c), increase monotonically with time and are similar for all vegetation classes. Although C_v determines the shape of the snowcover depletion curve during melt for an assumed lognormal distribution of pre-melt snow mass (Donald *et al.*, 1995; Shook, 1995), the standard deviation may be the more appropriate parameter for describing the development of a snowcover during redistribution by wind.

Snow surveys were carried out in open tundra, shrub tundra and forest areas on 23 April 1997; average snow masses and standard deviations are given in Table IV. The simulated snow mass for open tundra appears to be underestimated, but all model averages lie within one standard deviation of the survey results. A simulation with transport but no sublimation gives much greater snow accumulations than were measured — 141 $kg\ m^{-2}$ for open tundra, 270 $kg\ m^{-2}$ for shrub tundra and 608 $kg\ m^{-2}$ for forests — suggesting that sublimation is a significant component of the snow mass budget for TVC.

Topographic drifts surveyed at TVC, such as that shown in Figure 1, are generally too narrow to be resolved by the distributed model grid, but some topographic influence is evident in Figure 11, which shows average snow masses on open tundra as a function of aspect for slopes of greater and less than 9°. The accumulation is greatest on slopes in the lee of the dominant NW winds and least on windward slopes. Areas of shrub tundra are able to trap more snow than open tundra and show no strong relationship between snow accumulation and slope or aspect in the simulation.

The distribution of snow within each vegetation class is shown by snow mass frequency histograms in Figure 12. These distributions are not lognormal, but can be better approximated by sums of lognormals if

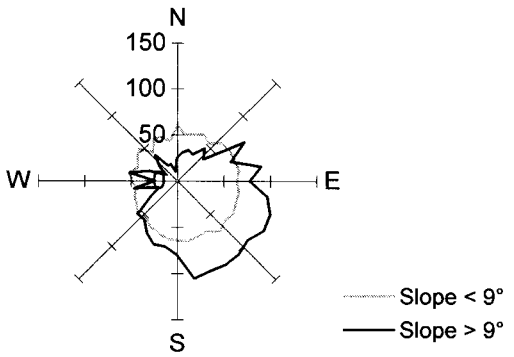

Figure 11. Average snow mass as a function of slope and aspect for open tundra from the simulation shown in Figure 9

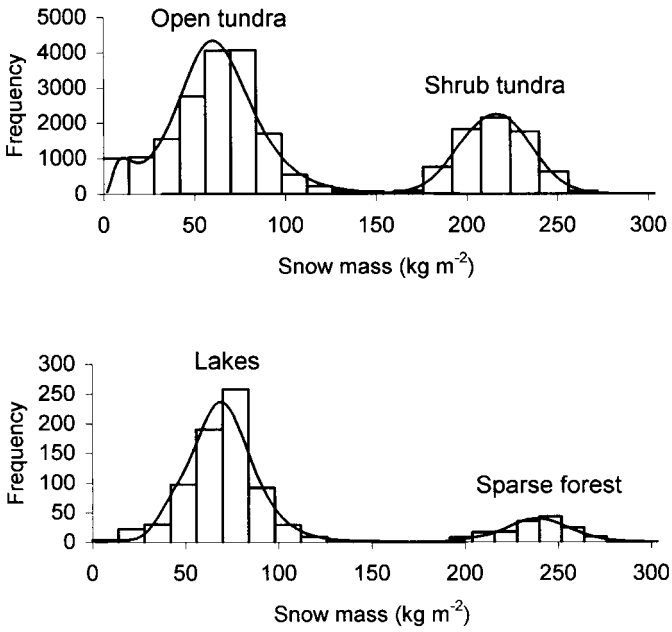

Figure 12. Snow mass frequency histograms for the simulation shown in Figure 9 compared with summed lognormal distributions

the vegetation classes are further partitioned according to landform. The landform classes used to categorize snow surveys in Table I are subjective, but they are intended to represent different windflow regimes. The curves in Figure 12 are sums of lognormals for five regimes classified directly from the simulation of NW windflow. For normalized windspeed $\hat{\boldsymbol{u}}$, the windflow regimes are:

Windswept — points with $|\hat{\boldsymbol{u}}| > 1{\cdot}06$ (local windspeeds exceeding the average by more than one standard deviation)
Windward — points at the windward edges of vegetation patches with transitions between short and tall vegetation
Divergent — points with $\nabla \cdot \hat{\boldsymbol{u}} > 10^{-4}$ m^{-1}
Convergent — points with $\nabla \cdot \hat{\boldsymbol{u}} < -10^{-4}$ m^{-1}
Neutral — all other points

Average snow masses and coefficients of variation for each regime are given in Table V for open tundra.

Average standard deviations of snow mass are plotted against sample length for north–south transects in Figure 13. The fitted lines are subjective, but suggest a power-law dependence with $H = 0{\cdot}27$ — close to the value obtained by Shook and Gray (1996) from TVC surveys, but larger than that calculated for the survey

Table V. Average snow masses and coefficients of variation for open tundra areas partitioned according to windflow regime

Windflow regime	Average snow mass (kg m^{-2})	C_v
Windswept	22	0·78
Windward	59	0·44
Divergent	61	0·32
Neutral	69	0·22
Convergent	76	0·30

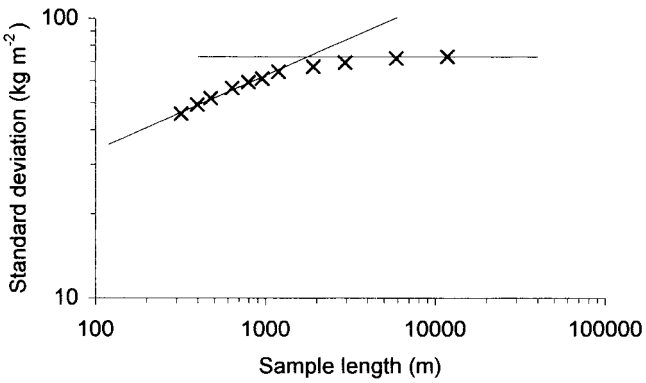

Figure 13. Average standard deviation of snow mass along north–south transects as a function of transect length for the simulation shown in Figure 9

shown in Figure 1 — and a 2 km cut-off, estimated from the intersection of the fractal slope and the asymptote. East–west transects give very similar results.

To investigate the sensitivity of the model to the representation of blowing snow development, a simulation was performed with full development ($F = 0$ in equation 16). This greatly increases the snow transport to forests, giving a final accumulation of 588 kg m^{-2}, and roughly doubles the coefficients of variation in snow mass for all vegetation classes, but has comparatively little influence on the Hausdorff dimension and cut-off length of the snow mass distribution.

CONCLUSIONS

A distributed model of blowing snow transport and sublimation has been developed and applied to an arctic basin. Simulated late-winter accumulations of snow for open tundra, shrub tundra and forest vegetation types compare reasonably well with measurements, provided sublimation processes are included; a simulation neglecting sublimation gives much greater accumulations than observed. The model is also able to reproduce several qualitative features of redistributed snowcovers found from snow surveys for windswept environments: vegetation has a strong control on snow accumulation, taller vegetation trapping more windblown snow and giving a smaller spatial variation in snow mass; distributions of snow mass can be approximated by lognormal distributions, provided areas are categorized according to vegetation cover and landform; the average standard deviation of snow mass along transects increases as a power of transect length up to a cut-off and approaches a constant value thereafter. Simulation results are sensitive to the representation used for the horizontal development of blowing snow, however; further work is required to develop a physically-based model of blowing snow development.

Despite simplifications introduced for efficiency, applying the distributed blowing snow model to a large area is computationally demanding. Scaling of blowing snow fluxes for large-scale modelling applications will be discussed in a following paper.

ACKNOWLEDGEMENTS

The authors acknowledge the support of: the Canadian GEWEX programme; the Canadian Climate Research Network, Land Surface Node; the Polar Continental Shelf Project, Dept of Natural Resources Canada; the Aurora Institute, Inuvik Research Laboratory, Government of the Northwest Territories; Water Resources Division, Dept of Indian and Northern Affairs Canada (Yellowknife); the National Hydrology Research Institute. Maintenance of field equipment and snow surveys were carried out by Cuyler Onclin, Newell Hedstrom, Tom Carter and Derek Faria. Trisalyn Nelson prepared the vegetation

classification. Natasha Neumann provided GIS and mapping assistance. R. E. is on leave from the Hadley Centre for Climate Prediction and Research, UK Meteorological Office.

REFERENCES

Bintanja R. 1998. The interaction between drifting snow and atmospheric turbulence. *Annals of Glaciology* **26**: 167–173.
Biöschl G. 1999. Scaling issues in snow hydrology. *Hydrological Processes* **13**: 2149–2175.
Déry SJ, Taylor PA, Xiao J. 1998. The thermodynamic effects of sublimating blowing snow in the atmospheric boundary layer. *Boundary-Layer Meteorology* **89**: 251–283.
Donald JR, Soulis ED, Kouwen N, Pietroniro A. 1995. A land cover-based snow cover representation for distributed hydrological models. *Water Resources Research* **31**: 995–1009.
Goodison BE, Metcalfe JR, Louie PYT. 1998. Summary of country analyses and results, Annex 5.B Canada. In *The WMO Solid Precipitation Measurement Intercomparison Final Report*, Instruments and Observing Methods Report No. 67, WMO, Geneva.
Jackson PS, Hunt JCR. 1975. Turbulent wind flow over a low hill. *Quarterly Journal of the Royal Meteorological Society* **101**: 929–955.
Lettau H. 1969. Note on aerodynamic roughness-parameter estimation on the basis of roughness element description. *Journal of Applied Meteorology* **8**: 828–832.
Li L, Pomeroy JW. 1997a. Estimates of threshold wind speeds for snow transport using meteorological data. *Journal of Applied Meteorology* **36**: 205–213.
Li L, Pomeroy JW. 1997b. Probability of occurrence of blowing snow. *Journal of Geophysical Research* **102**: 21955–21964.
Liston GE, Sturm M. 1998. A snow-transport model for complex terrain. *Journal of Glaciology* **44**: 498–516.
Mason PJ, Sykes RI. 1979. Flow over an isolated hill of moderate slope. *Quarterly Journal of the Royal Meteorological Society* **105**: 383–395.
Pomeroy JW. 1988. *Wind transport of snow*. Ph.D. Thesis, University of Saskatchewan.
Pomeroy JW, Gray DM, Landine PG. 1993. The Prairie Blowing Snow Model: characteristics, validation, operation. *Journal of Hydrology* **144**: 165–192.
Pomeroy JW, Gray DM. 1995. Snowcover accumulation, relocation and management. *National Hydrology Research Institute Science Report No. 7*, Environment Canada, Saskatoon: 134 p.
Pomeroy JW, Gray DM, Shook KR, Toth B, Essery RLH, Pietroniro A, Hedstrom N. 1998. An evaluation of snow accumulation and ablation processes for land surface modelling. *Hydrological Processes* **12**: 2339–2367.
Pomeroy JW, Li L. 1999a. Areal snowcover mass balance using a blowing snow model. I. Model structure. *Journal of Geophysical Research*. (submitted.)
Pomeroy JW, Li L. 1999b. Areal snowcover mass balance using a blowing snow model. II. Application to prairie and Arctic environments. *Journal of Geophysical Research*. (submitted.)
Pomeroy JW, Marsh P, Gray DM. 1997. Application of a distributed blowing snow model to the Arctic. *Hydrological Processes* **11**: 1451–1464.
Raupach MR, Gillette DA, Leys JF. 1993. The effect of roughness elements on wind erosion threshold. *Journal of Geophysical Research* **98**: 3023–3029.
Schmidt RA. 1982. Vertical profiles of windspeed, snow concentrations and humidity and humidity in blowing snow. *Boundary-layer Meteorology* **23**: 223–246.
Schmidt RA. 1991. Sublimation of snow intercepted by an artificial conifer. *Agricultural and Forest Meteorology* **54**: 1–27.
Shook K. 1995. Simulation of the ablation of prairie snowcovers. Ph.D. Thesis, University of Saskatchewan.
Shook K, Gray DM. 1996. Small-scale spatial structure of shallow snowcovers. *Hydrological Processes* **10**: 1283–1292.
Steppuhn H, Dyck GE. 1974. Estimating true basin snowcover. In *Advanced concepts and techniques in the study of snow and ice resources*. National Academy of Sciences: Washington, DC.: 314–328.
Takeuchi M. 1980. Vertical profiles and horizontal increases of drift snow transport. *Journal of Glaciology* **26**: 481–492.
Taylor PA, Walmsley JL, Salmon JR. 1983. A simple model of neutrally stratified boundary-layer flow over real terrain incorporating wavenumber-dependent scaling. *Boundary-Layer Meteorology* **26**: 169–189.
Thorpe AD, Mason BA. 1966. The evaporation of ice spheres and ice crystals. *British Journal of Applied Physics* **17**: 541–548.
Turcotte DL. 1992. *Fractals and Chaos in Geology and Geophysics*. Cambridge University Press: Cambridge.
Walmsley JL, Salmon JR, Taylor PA. 1982. On the application of a model of boundary-layer flow over low hills to real terrain. *Boundary-Layer Meteorology* **23**: 17–46.
Walmsley JL, Taylor PA, Keith T. 1986. A simple model of neutrally stratified boundary-layer flow over complex terrain with surface roughness modulations (MS3DJH/3R), *Boundary-Layer Meteorology* **36**: 157–186.

